Materials Research. 2017; 20(Suppl. 2): 910-916
DOI: http://dx.doi.org/10.1590/1980-5373-MR-2016-0969

Fibrous PCL/PLLA Scaffolds Obtained by Rotary Jet Spinning and Electrospinning

***Talita Almeida Vida*[a]*, *Adriana Cristina Motta*[b], *Arnaldo Rodrigues Santos Jr.*[c], *Guinea Brasil Camargo Cardoso*[a], *Crystopher Cardoso de Brito*[d], *Cecília Amélia de Carvalho Zavaglia*[a]**

[a]*Faculdade de Engenharia Mecânica, Universidade Estadual de Campinas, Campinas, SP, Brasil.*
[b]*Pontifícia Universidade Católica, São Paulo, SP, Brasil.*
[c]*Centro de Ciências Naturais e Humanas, Universidade Federal do ABC, Santo André, Brasil.*
[d]*Departamento de Ciências do Mar, Universidade Federal de São Paulo, Santos, SP, Brasil.*

Received: December 11, 2016; Revised: January 19, 2018; Accepted: February 07, 2018

Rotary jet spinning (RJS) and electrospinning are techniques to obtain fibrous scaffolds. RJS is a simple method, which fabricates three-dimensional fibers by exploiting a high-speed rotating nozzle, creating a polymer jet which stretches until solidification, and does not require high voltage. In opposite, electrospinning technique needs the presence of an external electric field to create fiber from the polymeric jet solution. This article investigates both processes using two different biocompatible polymers: Poly(L-lactic acid) (PLLA) and Poly(ε-caprolactone) (PCL). Samples were characterized by scanning electron microscopy, thermogravimetric analysis, differential scanning calorimeter, and Fourier-transform infrared spectroscopy. Morphological observations showed the efficiency of both techniques in obtaining nanofibers. Thermal analyses of data indicate immiscible property of different blends and the total solvent evaporation. In vitro cytocompatibility test showed that RJS and electrospinning samples exhibited good cytocompatibility. Based on these results, it may be concluded that the fibers obtained with both technologies are non-cytotoxicity and with good biocompatibility, and might be suitable for applications as scaffold for cell growth.

Keywords: *Rotary jet spinning, Electrospinning, Blend, Nanofibers, Biomaterials.*

1. Introduction

Since 1934, electrospinning has been used as an important method to obtain nano-/microfibers. It is based in the effect of electrostatic force on liquids, which spin polymer solutions or melts into whipped jets, producing continuous fibers with controlled diameter and orientation[1]. Electrospinning has different variations: solution, and melt electrospinning; solution electrospinning has wide techniques such as multi-jets from needle, multi-jets from multiple needles, and needleless systems. Indeed, despite many approaches, electrospinning still presents many drawbacks, mainly low productivity and electrical field requirements [2].

Rotary jet spinning (RJS) represents an available, cost effective process, and an efficient alternative method, with a 100-fold higher fiber production rate over that achievable by electrospinning. RJS also eliminates the requirement of an electric field or of a charged solution [3]. The system fabricates three-dimensional aligned or random nano-/microfibers by exploiting a high-speed rotating nozzle, to form a polymer jet that undergoes stretching before solidification [4].

Nano and microfibers have very wide applications on different fields; on tissue engineering they are investigated for vascular, bone, and epidermal applications. The structure is composed of fibers that may have different orientations, diameter, and materials, being interlaced or not.

This study focuses on the production of fibrous scaffolds using the RJS and electrospinning processes, aiming to compare the techniques, fibrous, and polymers. For such findings, fibrous scaffolds were produced using biocompatible polymers: poly(L-lactic acid) (PLLA) and poly(caprolactone) (PCL), in composition 50/50 %w/w. Samples were characterized by scanning electron microscopy (SEM), thermogravimetric analysis (TGA), differential scanning calorimeter (DSC), and Fourier-transform infrared spectroscopy (FTIR). Furthermore, an in vitro assay was produced to assess the biocompatibility of the samples.

2. Materials and Methods

2.1 Materials

PLLA (molecular weight 177.500 g/mol) was synthesized and provided by the Biomaterials Laboratory (PUC/SP Sorocaba), as described in a previous work [5]. PCL (molecular weight 70.000-90.000 g/mol) was purchased from Sigma Aldrich. The solvents were chloroform [$CHCl_3$, 99%] from Merck (Germany), and acetone [$(CH_3)_2CO$, 99.5%] from Synth (Brazil).

*vida85@fem.unicamp.br

2.2 Methods

PLLA and PCL (50/50 %w/w) were dissolved in a mixture of chloroform/acetone, to prepare the solutions at a 6% wt concentration. The solvents were used in two different compositions: a) only chloroform; b) polymers were first dissolved in chloroform and then added to 4:1 acetone. The mixtures were stirred for 2h for full homogenization, and for 12 hours before the use in RJS and electrospinning equipment. They were prepared with a total volume of 20 ml.

Rotary Jet Spinning equipment was built using low cost materials such as a sugar-cotton machine, as observed in Figure 1. To start the process, the collector was covered with a sheet of aluminum foil to facilitate the fiber collection. Prepared solution (blend/solvent) was slowly deposited, using a glass rod, to the central hole of the rotary reservoir at a 3450-rpm speed, and jets were expelled out from the four orifices. The jet, upon reaching the target, presents solvent evaporation, creating fibers and depositing them on the collector. The polymer solution was continuously fed into the reservoir at a sufficient rate to maintain a constant hydrostatic pressure and a continuous flow. This process uses centrifugal force to promote the fibers elongation, thus, rotating at a constant rotation speed takes from 1 to 2 minutes to produce the fibers.

Figure 1. Image of the rotary jet spinning equipment used (a) central reservoir, (b) circular target, (c) base coupled to an electric motor

Electrospinning equipment consists of a high-voltage source from 0 to 30 kV (Testtech), used to generate the electric field; a copper plate 90x70 mm; a capillary; and an infusion pump (KD-100, KD- Scientific), as observed in Figure 2. The system was initially assembled and then handled for the fiber production, the polymer solution being added to the capillary, consisting of a 20ml glass syringe, to a stainless-steel needle with 0.55mm of internal diameter. The syringe was placed in an infusion pump, which feeds the polymer solution to the needle tip at a flow rate of 1 ml/hr. The positive pole connector of the voltage source was positioned at the tip of the needle. The collector was then prepared, which consisted of a rectangular copper plate connected to the negative pole and the source, which was covered with a layer of aluminum foil to better collect the fibers. The target was positioned a fixed distance from the tip of the needle and from the 12cm collector. Finally, the system was switched on, using a voltage of 16 kV.

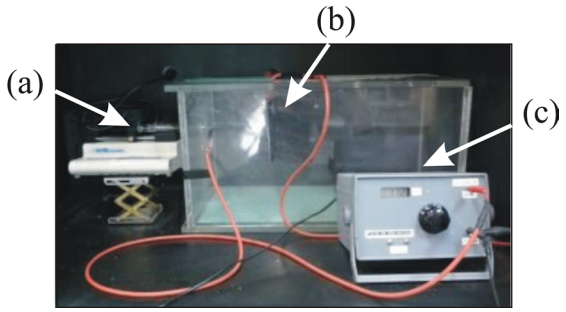

Figure 2. Image of the electrospinning equipment used (a) infusion pump, (b) metallic target, and (c) high-voltage source

2.3 Characterizations

Surface morphology of the meshes was characterized using Zeiss EVO MA-15 (operating mode, high vacuum, secondary electron SE detector) - the samples were gold coated, using the machine Sputter Coater (Bal-Tec SCD 050) with 40 mA, $5x10^{-7}$ Pa for 200 s. Fibers' dimensions were measured using the Image Tool software (UTHSCSA- Version 3.0); the average value was determined by measuring 50 fibers of each sample. The statistical analysis of the fiber diameter distribution was performed using Statistic 7.0 software. The samples' thermal properties were characterized by the DSC 200F3 Maia from the NETZSCH differential scanning calorimeter analyzer. The method for dynamic testing was performed within an atmosphere of liquid nitrogen 50 ml/min and two temperature scans in the following ranges: i) first scan from 25°C to 210°C, at a heating rate of 10°C/min and kept at that temperature for 5 minutes; ii) second scan was cooled to -100°C at a rate of 10°C/min for 5 minutes, and heated again to 210°C at a rate of 10°C/min. Thermal degradation data was obtained by the equipment STA409C (NETZSCH), as it charts mass (weight) vs. temperature (°C). The samples were heated from 25 to 600°C, at a heating rate of 10°C/min and a flow of 60 ml/min within a nitrogen atmosphere. The chemical changes in the different compositions were studied using Infrared Spectroscopy Fourier transforms (FTIR), Thermo Scientific - Nicolet 6700. The samples spectra were assessed using an average wavelength scan from 675 to 4000 cm^{-1}.

Fibroblastic cell line- and Vero cells- were used in this research, obtained from the Adolfo Lutz Institute, São Paulo, Brazil, and established from the kidney of an African green monkey (*Cercopithecus aethiops*). The cells were cultured in Medium 199 (Lonza Group Ltd, USA) and supplemented with 10% fetal calf serum (FCS, by Nutricell Nutrientes Celulares, Campinas, SP, Brazil), at a temperature of about

37ºC. Vero cells are recommended for cytotoxicity and cell-substratum interactions studies, with biomaterial researches [6,7]. The concentration of 1x105cells/ml was inoculated on 24-well culture plates (Corning) on the different biomaterial compositions. After 120 hours in culture, the samples were fixed with paraformaldehyde 4% (in phosphate buffer 0.1M, pH 7.2) or ethanol/acetic acid (3/1), and stained with Cresyl Violet (CV) or Toluidine Blue (TB) at pH 4.0, respectively. The control group comprised other cells cultured on a culture plate. All experiments were done in triplicate. Images of the samples were obtained through the Olympus IX-50 inverted microscope.

An indirect cytotoxicity assay was performed. The extracts were obtained by added material samples in Medium 199 (Lonza) with 10% FCS (Nutricell), at a final concentration of 0.2 g/ml, and then incubated at 37ºC for 24 h. After this period, the medium harvested and the materials were discarded. Vero cell suspension containing 1x105cells/ml in Medium 199 with 10% FCS were transferred to a 96-well culture plate (Corning Co., Cambridge, MA, USA) and cultured for 2 h at 37°C. After this incubation time, the medium was removed, and the cells were incubated with biomaterial extracts. The cells were cultured by 24h in these culture conditions, according to Mosmam's Methodology. The wells were washed twice with 0.1M phosphate buffered saline (PBS), pH 7.4, at 37°C, and incubated with 100µL of FCS-free Medium199. The assay mixture (10µL per well) containing 5mg/mL of 3-(4.5-dimetiltiazol-2-il)-2.5 diphenyl tetrazolium bromide (MTT, Sigma-Aldrich/USA) was added to each well and incubated in the dark at 37°C. After 4h, SDS (Sigma) was added to each well, and 12 hours later the cells were quantified at 540nm by using multi scan microplatereader.

The results are expressed as mean ± ST. Comparisons between groups were made using ANOVA, followed by Tukey's correction factor for multiple comparisons as a *post-hoc* test.

3. RESULTS

3.1 Morphology

To observe the morphological aspects from the obtained fibrous, SEM analysis was carried out on samples of RJS and electrospinning. Figure 3 shows the composition of 50% PLLA/PCL, using the both solvent compositions. Likewise, the measurement of the fibers' diameter is observed in the Table 1.

Table 1 summarizes the mean fiber diameter for both processes. Fibers obtained by electrospinning have a lower value when compared with the RJS fibers. Different diameters may be suitable for application on tissue engineering. Large diameter fibers can provide the structural stability and mechanical properties required for support, whereas the small diameter fibers can provide a suitable environment for the cells to attach to the support structure [8].

3.2 Thermal analysis

All the different composition samples featured as semi-crystalline polymers since the curves show the presence of Tg (in the first and second heating), crystallization peaks (in the cooling, first, and second heating), and melting (in the first and second heating), as observed on Figure 4.

Samples that had only chloroform as solvent presented some characteristics in common: the first heating of the DSC curve showed two melting peaks (Tm), corresponding to PLLA and PCL, and glass transition temperature (Tg) for PLLA. For the pure polymers the Tm was ~180 °C and ~64 °C, PLLA and PCL respectively. The melting peak of the 1st heating is wider; however, in the 2nd heating, the peak is elongated and at a lower temperature due to the crystal sizes distribution - which is a secondary crystallization characteristic that occurs during cooling. It was also observed that, in the 2nd heating, the Tg of the PLLA by electrospinning had smaller values, ~60 °C, and ~ -64 °C for PCL; by rotary jet spinning it was ~59 ° C and ~-64 °C, for PLLA and PCL, respectively. A peak, indicative of crystallization and melting, was also observed for PLLA. For PCL, only a melting peak was observed. Also, concerning the glass transition temperature (Tg) of the PLLA, it was observed that a slight increase occurred in the values with the addition of PCL in the blend. The Tg, therefore, did not suffer that much variation regarding the compositions of the polymer in the blends, which indicates the blend immiscibility. With the curves was possible to verify small or no changes in the values of Tg, Tc, and Tm in the different samples.

Interestingly, when acetone/chloroform were used as solvents, it had alterations: PLLA/PCL- electrospinning sample presented a Tm reduction and Tc peaks during the first heating, as well as on the second peak, and an increase of $Tm_{pcl.}$ Those modifications were due to the process and evaporation rate of the solvents− which induce the crystallization of the polymers.

To assess the compositions stability, thermal degradation was produced using thermogravimetric analysis (TGA) - Table 2. PLLA and PCL samples without processing were compared to the samples of both processes. TGA results indicate that both processes evaluated in this article did not alter the thermal property. Pure PLLA and PCL, as well as the processed ones, presented mean values of initial degradation temperature of 340 ºC and 387 ºC, respectively. Mass loss values for the two polymers are close to the values found in the literature [5,9].

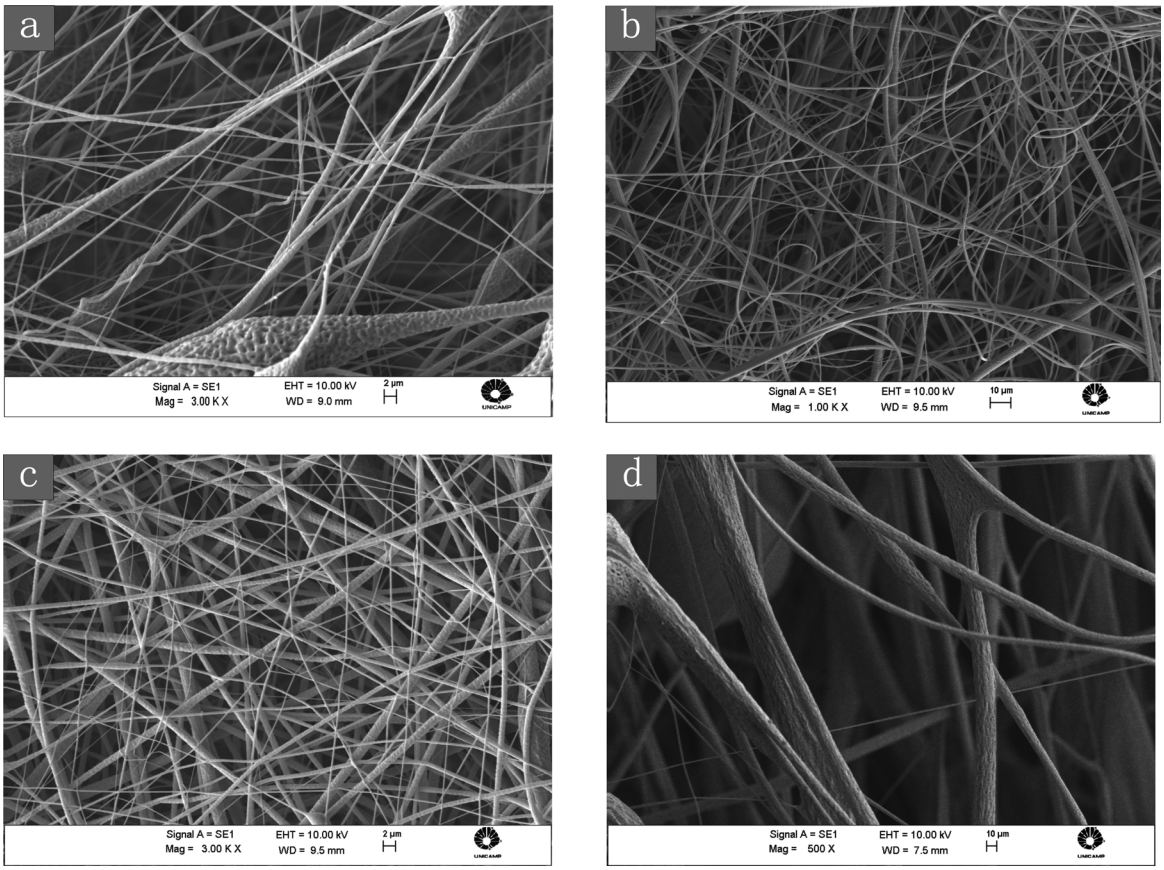

Figure 3. SEM micrographs of different solvents compositions by electrospinning and rotary jet spinning: (a) and (b) Chloroform: (c) and (d) Chloroform/Acetone

Table 1. Fibers' diameters of electrospinning and rotary jet spinning processes.

Composition PLLA/PCL (%)	Electrospinning		Rotary Jet Spinning	
	Chloroform	Chloroform +Acetone	Chloroform	Chloroform +Acetone
	Mean (nm)		Mean (nm)	
50	717 ± 273	639 ± 374	1647 ± 976	8002 ± 5051

Both techniques may cause alterations on the molecular behavior of the compositions (Figure 5). It is possible to observe the correlation of intensity and concentration: the 2996 cm^{-1} peak for PLLA, which corresponds to the asymmetric stretching of CH3 (ν CH3) [10], shows a more intense peak in the pure PLLA sample, and decreased the spectrum intensity for such sample (50/50).

The 2947 cm^{-1} peak is observed for both PLLA and PCL. This peak is shorter in the PLLA spectrum than in the blend, and the PCL spectrum is more evident. This peak is approached as a symmetric stretch of CH_3 [10] (νCH_3) of PLLA. For the PCL, the vibration belongs to the asymmetric stretch of CH_2 (νCH_2) [11]. A weak peak at 2882 cm^{-1} of the PLLA is identified as corresponding to the CH stretch [10] that is absent in the blends' spectra. PCL sample shows a narrow peak at 2867 cm^{-1}, which belongs to the symmetrical CH_2 stretch (νCH_2) [11]. This peak shows a slight intensity reduction on the blends. All peaks shown in the frequency region between 3100 and 2750 cm^{-1} did not change for different processes and solutions.

Other characteristic peak of each polymer was in the region 2000 to 675 cm^{-1} and 1456 cm^{-1} , correspondent to the PLLA present in the two chloroform-processes' spectra; 1454 cm^{-1} for the processes using chloroform and acetone; and 1471 cm^{-1} for PCL peak that belong to the asymmetric CH_3 stretch and the CH_2 scissors, respectively. In this case, the vibration at 1471 cm^{-1} is completely "absorbed" in the blends by the 1456 cm^{-1} peak of the PLLA. Other characteristic peaks of the PLLA is 1209 cm^{-1}, corresponding to the C-C bond, and 1185 cm^{-1}, corresponding to the axial strain band of the C-O-C bond, which, in the case of the polymeric structure, behaves as a C-O-C complex of ethers ($_{\nu}$COC),

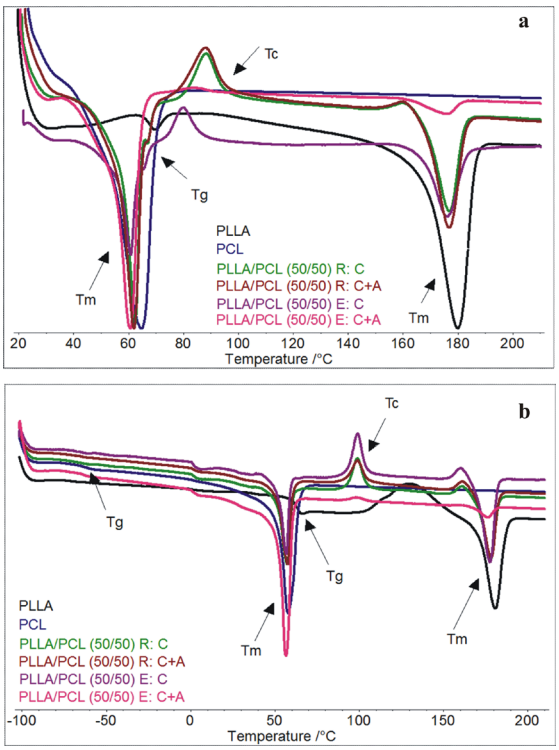

Figure 4. DSC graphics: (a) first heating and (b) second heating. Samples obtained by electrospinning and rotary jet spinning using different solvent compositions

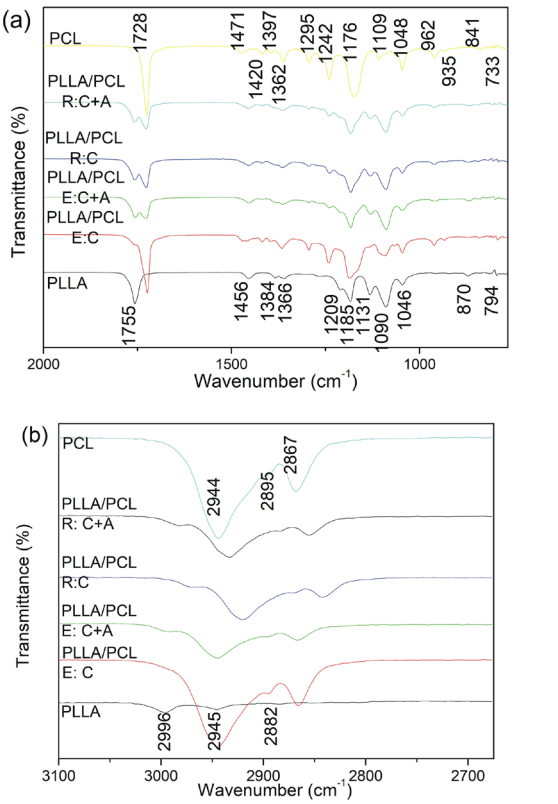

Figure 5. Spectrum of the samples obtained by electrospinning (E) and rotary jet spinning (R), using chloroform (C) and chloroform/acetone (C+A): (a) high wavelength, lower wavelength from 2000 to 675 cm^{-1}, and (b) 3100 to 2750 cm^{-1}

Table 2. Degradation temperature of different samples using chloroform and chloroform/acetone on electrospinning and rotary jet spinning processes.

CompositionPLLA/PCL (%)	Electrospinning		Rotary Jet Spinning		Electrospinning		Rotary Jet Spinning	
	PLLA	PCL	PLLA	PCL	PLLA	PCL	PLLA	PCL
	Chloroform		Chloroform/Acetone		Chloroform		Chloroform/Acetone	
	Ti (ºC)	Ti (ºC)	Ti (ºC)	Ti (ºC)	Ti (ºC)	Ti(ºC)	Ti (ºC)	Ti (ºC)
PLLA	340	-	340	-	340	-	340	-
(50/50)	338	391	324	390	340	390	345	390
PCL	-	387	-	387	-	387	-	387

with asymmetric axial deformation [12]; this last peak for PCL appears at 1242 cm^{-1}. Also for the PCL, the peak at 1176 cm^{-1} occurs, which corresponds to the symmetrical C-O-C (νCOC) stretch.

To observe the growth of the cells, they were stained with toluidine blue (TB) and cresyl violet (CV). TB staining is a basophilic dye that, in pH 4.0, is used for cytochemistry detection of DNA, RNA, and glycosaminoglycans. Basophils indicate if a cell exhibit a great amount of RNA, thus indicating cell activity. CV is a dye used for cellular morphology. In figure 6, it is possible to observe the cultured cells in PLLA/PCL samples with different solvent choices. A more intensely stained, light metachromatic cytoplasmic basophil, with the largest number of cells, was observed in all of them. The same TB may show SO4 and COO groups, present only in glycosaminoglycans. For a longer-period assay, it was evaluate using the MTS test; therefore, it was possible to observe a high proliferation on the composition used, indicating the blend biocompatibility.

4. Discussions

Electrospinning is the most common method for nanofibers production, even if this method is used since 1934 and still suffers from many drawbacks such as low productivity and the need of electrical fields. The rotary jet spinning technique is a new process, which achieve aligned fibers samples using a high-speed rotation of polymer solution jets to extrude three-dimensional nanofibers structures [3]. The major advantages when comparing RJS with the electrospinning

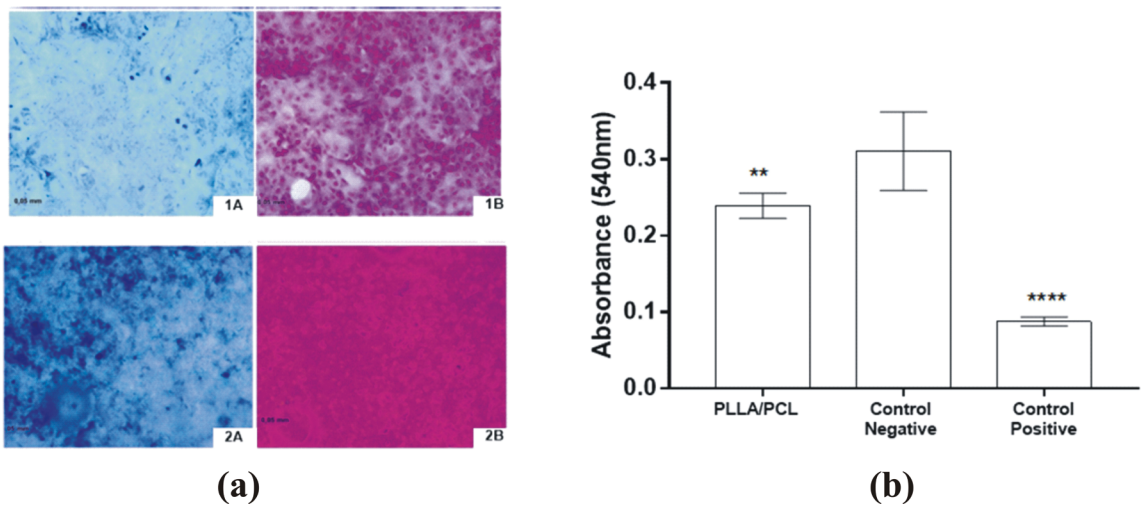

Figure 6. In vitro assay with (a) 2 days of culture: (A) TB staining, (B) CV staining on (1) PLLA/PCL using chloroform as solvent, and (2) PLLA/PCL using chloroform/acetone as solvent; and (b) 5 days of culture

are the absence of electric field; higher production rate, e.g. 2 g min $^{-1}$ in comparison with 0.02 g h^{-1}[13]; elimination of the need for a charged solution, allowing more materials to be tested - materials that were not used due to the low dielectric constants; and its applicability to polymeric emulsions and suspensions [2]. In this article we compare the results of different compositions using the RJS and electrospinning techniques.

Based on the analysis of SEM images, the samples had porous, interconnected, and fibrous structures. However, the morphology of each sample showed differences in the diameter of the fibers: PLLA / PCL blends (50/50) showed beads in the chloroform-dissolved fiber structure obtained by electrospinning (Figure 3a). According to Perea [14], the formation of these beads can occur due to instabilities in the jet during the process, generating changes in the solution physical properties such as viscosity and surface tension. Figure 3c shows the SEM micrograph of the chloroform-dissolved RJS sample, indicating porous fibrous structures, with no beads and a noteworthy formation of fibers in network structures, which may be a consequence of the short distance between the central reservoir and the circular collector, and of the speed with which the solution is expelled from the reservoir. In the fibers obtained by electrospinning using chloroform/acetone the sample was irregular due to the randomness with which the fibers are formed on the collector and also to the absence of beads, as shown in Figure 3b. Figure 3d shows the micrographs of the samples prepared by chloroform/acetone RJS samples, a typical morphology of irregular fibers and fibers with little or no appearance of beads was observed; possibly this fact can be attributed to the process, i.e., the rapid rate of the fiber ejection and formation.

Fibers' diameter were correlated to solvent and process (Table 1). Samples by electrospinning had lower mean when compared with those by rotary jet spinning process. In terms of solvent choice, it only interfered on the RJS process, due to the fact this technique depends of exploiting a high-speed rotation nozzle to form a polymer jet, therefore, viscosity and solvent rate highly influences on the result.

It was also possible to verify that, regardless of the applied process (electrospinning and RJS), and of the solvent used (chloroform and chloroform/acetone) there was no significant variation in the polymer properties, which was confirmed by the thermal analysis; the compositions demonstrate the immiscibility of the polymers, as well as structure stability after the processes (Figure 4 and Table 2). Also, using different analysis was able to identify chemical bonds and correlations between the two polymers used (Figure 5).

In addition, fibrous scaffolds need to present an ideal structure, likewise replicate complex external shapes. Therefore, the ability to control scaffold architecture, material composition, and porosity throughout the design and fabrication could be a critical factor in the future clinical success of tissue engineering. An ideal for tissue engineering should be, thus, to combine design and automated manufacturing techniques to enable patient specific implants and tissue reconstruction strategies.

Furthermore, biocompatibility is an extremely important topic. It was cultured with Vero cells in vitro, for 24 hours, to investigate the initial behavior of cells to the substrates; and 5 days to investigate the cellular grown (Figure 6). Indirect in vitro assay was performed to evaluate the biocompatibility of the compositions; during the 24 initial hours, there was no significant difference of cell proliferation between the samples. The proliferation assay was performed by evaluating carbohydrates and proteins cytochemically. We observed, in all studies samples, the presence of spreading cells on the substrates, usually with decondensed chromatin and evident nucleolus. A confluent cell layer can be seen on the

various polymers studied, indicating that cells proliferate on the samples. Indeed, after 5 days of culture, we were able to investigate the effects of the biomaterials on animal cells, indicating the possibility of different applications due to the compatible surface, which is one of the prerequisites for implantations.

5. Conclusions

To a successful scaffold, a correct structure must be planned, to reach tissue similarly. Until now, fabrication methods have demonstrated scaffolds in polymeric or polymer-ceramic composites, with limited control over geometry and porosity. It is known that scaffold materials and pore morphology significantly influence the tissue regeneration since they induce cellular adhesion and proliferation [15]. In this article, we demonstrate two different techniques to obtain fibrous scaffolds, and the influences of each process on the sample obtained.

Scanning electron microscopy analyzes showed that both processes were successful in fiber formation. Nano and microfibers presented different morphologies depending on the solvent, polymeric composition, and processes. In all the compositions the solvents choice and/or process did not caused alteration on the polymeric properties: all demonstrated blends immiscibility, and thermal and molecular stability. In addition, in vitro assays assessed biocompatibility and scaffold viability for using them as fibrous scaffolds for tissue engineering.

6. Acknowledgements

The authors gratefully acknowledge financial support provided by CAPES, FAPESP (grant 2013/19372-0), Biofabris-INCT and Biomaterials Laboratory PUC/SP Sorocaba.

7. References

1. Cardoso GBC, Perea GNR, D'Avila MA, Dias CGBT, Zavaglia CAC, Arruda ACF. Initial Study of Electrospinning PCL/PLLA Blends. *Advances in Materials Physics and Chemistry*. 2011;1(3):94-98.

2. Nayak R, Padhye R, Kyratzis IL, Truong YB, Arnold L. Recent advances in nanofibre fabrication techniques. *Textile Research Journal*. 2011;82(2):129-147.

3. Badrossamay MR, Balachandran K, Capulli AK, Golecki HM, Agarwal A, Goss JA, et al. Engineering hybrid polymer-protein super-aligned nanofibers via rotary jet spinning. *Biomaterials*. 2014;35(10):3188-3197.

4. Cardoso GB, Machado-Silva AB, Sabino M, Santos AR Jr, Zavaglia CA. Novel hybrid membrane of chitosan/poly (e-caprolactone) for tissue engineering. *Biomatter*. 2014;4. pii: e29508.

5. Motta ACMM. *Síntese e caracterização do Poli(l-ácido láctico)-PLLA e Poli(L-ácido láctico-co-ácido glicólico)-PLGA e estudo da degradação "in vitro"*. [Thesis]. Campinas: University of Campinas; 2002.

6. *Use of International Standard ISO- 10993, "Biological Evaluation of Medical Devices Part 1: Evaluation and Testing" - Draft Guidance for Industry and Food and Drug Administration Staff*. Rockville: U.S. Department of Health and Human Services; Food and Drug Administration; Center for Devices and Radiological Health; Office of Device Evaluation; 2013.

7. Santos AR Jr, Barbanti SH, Duek EAR, Wada MLF. Analysis of the growth pattern of Vero cells cultured on dense and porous poly (L-Lactic Acid) scaffolds. *Materials Research*. 2009;12(3):257-263.

8. Huttunen M, Kellomäki M. A simple and high production rate manufacturing method for submicron polymer fibres. *Journal of Tissue Engineering and Regenerative Medicine*. 2011;5(8):e239-243.

9. Ramos SLF.*Membranas de policaprolactona obtidas por eletrofiação para utilização em engenharia tecidual*. [Thesis]. Campinas: University of Campinas; 2011.

10. Porwal V, Singh D, Chatruvedi D, Tandon P, Gupta VD. Vibrational dynamics and heat capacity in poly(L-lactic acid). *Journal of Polymer Science Part B Polymer Physics*. 2010;48(2):175-182.

11. Misra RM, Agarwal R, Tandon P, Gupta VD. Phonon dispersion and heat capacity in poly(e-caprolactone). *European Polymer Journal*. 2004;40(8):1787-1798.

12. Simões MS. *Desenvolvimento e estudo in vitro de implante biorreabsorvível em poli (l-lactídeo) (PLLA) para artrodese de coluna lombar*. [Dissertation]. Porto Alegre: Pontifical Catholic University of Rio Grande do Sul; 2007.

13. Weng B, Xu F, Lozano K. Mass production of carbon nanotube-reinforced polyacrylonitrile fine composite fibers. *Journal of Applied Polymer Science*. 2014;131(11):40302.

14. Rodríguez Perea GN. *Eletrofiação de nanocompósito de poli(L-ácido lático) com hidroxiapatita para regeneração óssea*. [Thesis]. Campinas: University of Campinas; 2011.

15. Hasirci V, Pepe-Mooney BJ. Understanding the cell behavior on nano-/micro-patterned surfaces. *Nanomedicine (Lond)*. 2012;7(9):1375-1389.